



LOWER BOUND FOR THE EXPECTED SUPREMUM OF FRACTIONAL BROWNIAN MOTION USING COUPLING

KRZYSZTOF BISEWSKI ,* *Université de Lausanne*

Abstract

We derive a new theoretical lower bound for the expected supremum of drifted fractional Brownian motion with Hurst index $H \in (0, 1)$ over a (in)finite time horizon. Extensive simulation experiments indicate that our lower bound outperforms the Monte Carlo estimates based on very dense grids for $H \in (0, \frac{1}{2})$. Additionally, we derive the Paley–Wiener–Zygmund representation of a linear fractional Brownian motion in the general case and give an explicit expression for the derivative of the expected supremum at $H = \frac{1}{2}$ in the sense of Bisewski, Dębicki and Rolski (2021).

Keywords: Fractional Brownian motion; expected value of supremum; expected workload; lower bound

2020 Mathematics Subject Classification: Primary 60G22
Secondary 60G15; 68M20

1. Introduction

Let $\{B_H(t), t \in \mathbb{R}_+\}$, where $\mathbb{R}_+ := [0, \infty)$, be fractional Brownian motion with Hurst index $H \in (0, 1)$ (or H -fBm), that is, a centred Gaussian process with the covariance function $\text{Cov}(B_H(t), B_H(s)) = \frac{1}{2}(s^{2H} + t^{2H} - |t - s|^{2H})$, $s, t \in \mathbb{R}_+$. In this manuscript we consider the expected supremum of fractional Brownian motion with drift $a \in \mathbb{R}$ over time horizon $T > 0$, i.e. $\mathcal{M}_H(T, a) := \mathbb{E}(\sup_{t \in [0, T]} B_H(t) - at)$. Even though the quantity $\mathcal{M}_H(T, a)$ is so fundamental in the theory of extremes of fractional Brownian motion, its value is known explicitly only in two cases: $H = \frac{1}{2}$ and $H = 1$, when B_H is a standard Brownian motion and a straight line with normally distributed slope, respectively. For general $H \in (0, 1)$, the value of $\mathcal{M}_H(T, a)$ could, in principle, be approximated using Monte Carlo methods by simulation of fractional Brownian motion on a dense grid, i.e. $\mathcal{M}_H^n(T, a) := \mathbb{E}(\sup_{t \in \mathcal{T}_n} \{B_H(t) - at\})$, where $\mathcal{T}_n := \{0, T/n, 2T/n, \dots, T\}$. However, this approach can lead to substantial errors. In [8, Theorem 3.1] it was proven that the absolute error $\mathcal{M}_H(T, 0) - \mathcal{M}_H^n(T, 0)$ behaves roughly (up to logarithmic terms) like n^{-H} as $n \rightarrow \infty$. This becomes problematic as $H \downarrow 0$, when additionally $\mathcal{M}_H(T, 0) \rightarrow \infty$; see also [17]. Similarly, the error is expected to be large when T is large, since in that case more and more points are needed to cover the interval $[0, T]$. Surprisingly, even as $H \uparrow 1$ we may also encounter problems because then $\mathcal{M}_H(\infty, a) \rightarrow \infty$ for all $a > 0$; see [4, 18]. Since the estimation of $\mathcal{M}_H(T, a)$ is so challenging, many works are dedicated to finding its theoretical upper and lower bounds. The most up-to-date bounds for $\mathcal{M}_H(T, 0)$ can be found in [8, 9]; see also [23, 26] for older results. The most up-to-date bounds for $\mathcal{M}_H(\infty, a)$ can be found in [4].

Received 25 January 2022; revision received 11 November 2022.

* Postal address: Quartier UNIL-Chamberonne, Bâtiment Extranef, 1015 Lausanne, Switzerland.

© The Author(s), 2023. Published by Cambridge University Press on behalf of Applied Probability Trust.

In this work we present a new theoretical lower bound for $\mathcal{M}_H(T, a)$ for general $T > 0$, $a \in \mathbb{R}$ (including the case $T = \infty$, $a > 0$). Our approach is loosely based on recent work [5], where the authors consider a coupling between H -fBMs with different values of $H \in (0, 1)$ on the Mandelbrot–van Ness field [19]. By a coupling we mean that H -fBMs live in the same probability space and have a non-trivial joint distribution. The idea of considering such a coupling dates back to at least [3, 20], which introduced a so-called multi-fractional Brownian motion. In this manuscript we consider a coupling provided by the family of linear fractional stable motions with $\alpha = 2$, see [21, Chapter 7.4], which we will call linear fractional Brownian motion. Conceptually, our bound for $\mathcal{M}_H(T, a)$ is very simple: it is defined as the expected value of the H -fBm at the time of the maximum of the corresponding $\frac{1}{2}$ -fBm (i.e. Brownian motion). The difficult part is the actual calculation of this expected value. This is described in detail in Section 3. Our new lower bound, which we denote by $\underline{\mathcal{M}}_H(T, a)$, is introduced in Theorem 1.

Our numerical experiments show that $\underline{\mathcal{M}}_H(T, a)$ performs exceptionally well in the sub-diffusive regime $H \in (0, \frac{1}{2})$. In fact, the numerical simulations indicate that $\underline{\mathcal{M}}_H(T, a)$ gives a *better approximation* to the ground truth than the Monte Carlo estimates with as many as 2^{16} gridpoints, i.e. $\underline{\mathcal{M}}_H(T, a) \geq \mathcal{M}_H^n(T, a)$, $n = 2^{16}$, for all $H \in (0, \frac{1}{2})$. We emphasise that $\underline{\mathcal{M}}_H(T, a)$ is the theoretical *lower bound* for $\mathcal{M}_H(T, a)$, which makes the result above even more surprising.

The manuscript is organised as follows. In Section 2 we define linear fractional Brownian motion and establish its Paley–Wiener–Zygmund representation. We also recall the formula for the joint density of the supremum of drifted Brownian motion and its time, and introduce a certain functional of the three-dimensional Bessel bridge, which plays an important role in this manuscript. In Section 3 we show our main results; our lower bound $\underline{\mathcal{M}}_H(T, a)$ is presented in Theorem 1 in a general case. Explicit values of $\underline{\mathcal{M}}_H(T, a)$ are provided in Corollary 2. Additionally, in Theorem 2 we present an explicit formula for the derivative $(\partial/\partial H)\mathcal{M}_H(T, a)|_{H=1/2}$, which was given in terms of a definite integral in [5]. The main results are compared to numerical simulations in Section 4, where the results are also discussed. The proofs of the main results are given in Section 5. In Appendix A we recall the definition and properties of confluent hypergeometric functions. Finally, in Appendix B (available in the Supplementary Material of the online version of this article) we include various calculations needed in the proofs.

2. Preliminaries

2.1. Linear fractional Brownian motion

In this section we introduce the definition of linear fractional Brownian motion and establish its Paley–Wiener–Zygmund representation.

Let $\{B(t) : t \in \mathbb{R}\}$ be a standard two-sided Brownian motion. For $(H, t) \in (0, 1) \times \mathbb{R}_+$ let

$$\begin{aligned}
 X_H^+(t) &:= \int_{-\infty}^0 [(t-s)^{H-(1/2)} - (-s)^{H-(1/2)}] dB(s) + \int_0^t (t-s)^{H-(1/2)} dB(s), \\
 X_H^-(t) &:= - \int_0^t s^{H-(1/2)} dB(s) - \int_t^\infty [s^{H-(1/2)} - (s-t)^{H-(1/2)}] dB(s).
 \end{aligned}
 \tag{1}$$

Note that in case $H = \frac{1}{2}$ we have $X_{1/2}^+(t) = B(t)$, $X_{1/2}^-(t) = -B(t)$. Furthermore, for $\mathbf{c} := (c_+, c_-) \in \mathbb{R}_0^2$, with $\mathbb{R}_0^2 := \mathbb{R}^2 \setminus \{(0, 0)\}$, put

$$X_H^c(t) := c_+X_H^+(t) + c_-X_H^-(t). \tag{2}$$

Finally, for any $\mathbf{c} \in \mathbb{R}_0^2$, we define the (standardised) linear fractional Brownian motion $\{B_H^c(t) : (H, t) \in (0, 1) \times \mathbb{R}_+\}$, where

$$B_H^c(t) := \frac{X_H^c(t)}{\sqrt{V_H^c}}, \quad V_H^c := \text{Var}X_H^c(1). \tag{3}$$

Now, according to [25, Lemma 4.1] we have

$$V_H^c := C_H^2 \cdot \left[\left((c_+ + c_-) \cos\left(\frac{1}{2}\pi\left(H + \frac{1}{2}\right)\right) \right)^2 + \left((c_+ - c_-) \sin\left(\frac{1}{2}\pi\left(H + \frac{1}{2}\right)\right) \right)^2 \right], \tag{4}$$

where

$$C_H^2 := \frac{\Gamma\left(\frac{1}{2} + H\right)\Gamma(2 - 2H)}{2H\Gamma\left(\frac{3}{2} - H\right)}. \tag{5}$$

We emphasise that $B_H(t)$ is a Gaussian field with well-known covariance structure, i.e. for each $\mathbf{c} \in \mathbb{R}_0^2$, the value of

$$\text{Cov}(B_{H_1}^c(t_1), B_{H_2}^c(t_2)), \quad (H_1, t_1), (H_2, t_2) \in (0, 1) \times \mathbb{R}_+^2, \tag{6}$$

is known, see [25, Theorem 4.1]. While for each $H \in (0, 1)$, the process $\{B_H^c(t) : t \in \mathbb{R}_+\}$ is an H -fBm (therefore its law is independent of the choice of the pair \mathbf{c}), the covariance structure (6) of the entire field varies for different \mathbf{c} ; see [25]. In other words, different choices of \mathbf{c} will provide different couplings between the fractional Brownian motions. The case $\mathbf{c} = (1, 0)$ corresponds to the fractional Brownian field introduced by Mandelbrot and van Ness in [19] (note that in this case we have $V_H^c = C_H^2$). We remark that the representation (3) was recently rediscovered in [15].

Following [5], we use the *Paley–Wiener–Zygmund* (PWZ) representation of processes $\{\tilde{X}_H^+(t) : (H, t) \in (0, 1) \times \mathbb{R}_+\}$ and $\{\tilde{X}_H^-(t) : (H, t) \in (0, 1) \times \mathbb{R}_+\}$ defined in (1),

$$\begin{aligned} \tilde{X}_H^+(t) &= t^{H-(1/2)} \cdot B(t) - \left(H - \frac{1}{2}\right) \cdot \int_0^t (t-s)^{H-(3/2)} \cdot (B(t) - B(s)) \, ds \\ &\quad + \left(H - \frac{1}{2}\right) \cdot \int_{-\infty}^0 [(t-s)^{H-(3/2)} - (-s)^{H-(3/2)}] \cdot B(s) \, ds, \\ \tilde{X}_H^-(t) &= -t^{H-(1/2)} \cdot B(t) + \left(H - \frac{1}{2}\right) \cdot \int_0^t s^{H-(3/2)} \cdot B(s) \, ds \\ &\quad + \left(H - (1/2)\right) \cdot \int_t^\infty [s^{H-(3/2)} - (s-t)^{H-(3/2)}] \cdot (B(s) - B(t)) \, ds. \end{aligned} \tag{7}$$

Proposition 1. $\{\tilde{X}_H^\pm(t) : (H, t) \in (0, 1) \times \mathbb{R}_+\}$ is a continuous modification of $\{X_H^\pm(t) : (H, t) \in (0, 1) \times \mathbb{R}_+\}$.

Now let us define the counterpart of the process $X_H^c(t)$ from (2), i.e., for every $\mathbf{c} := (c_+, c_-) \in \mathbb{R}_0^2$ define the stochastic process $\{\tilde{X}_H^c(t) : (H, t) \in (0, 1) \times \mathbb{R}_+\}$, where

$$\tilde{X}_H^c(t) = c_+\tilde{X}_H^+(t) + c_-\tilde{X}_H^-(t). \tag{8}$$

Corollary 1. $\{\tilde{X}_H^c(t) : (H, t) \in (0, 1) \times \mathbb{R}_+\}$ is a continuous modification of $\{X_H^c(t) : (H, t) \in (0, 1) \times \mathbb{R}_+\}$.

Corollary 1 generalises [5, Proposition 4.1] in the case $n = 0$. For completeness, we give a short proof of Proposition 1 below.

Proof of Proposition 1. In [5, Proposition 4.1] it was shown that $\{\tilde{X}_H^+(t) : (H, t) \in (0, 1) \times \mathbb{R}_+\}$ is a continuous modification of $\{X_H^+(t) : (H, t) \in (0, 1) \times \mathbb{R}_+\}$. Showing the sample path continuity of $\{\tilde{X}_H^-(t) : (H, t) \in (0, 1) \times \mathbb{R}_+\}$ is analogous to showing the sample path continuity of \tilde{X}^+ , which was done in [5, Proposition 4.2]. Finally, due to [5, Lemma A.1], for any $(H, t) \in (0, 1) \times \mathbb{R}_+$ we have $\tilde{X}_H^-(t) = X_H^-(t)$ almost surely (a.s.). This shows that \tilde{X}^- is a modification of X^- and concludes the proof. \square

2.2. Joint density of the supremum of drifted Brownian motion and its time

In this section we recall the formulae for the joint density of the supremum of (drifted) Brownian motion over $[0, T]$ and its time due to [24]. This section relies heavily on [5, Section 2].

Let $\{B(t) : t \in \mathbb{R}_+\}$ be a standard Brownian motion. For any $T > 0$ and $a \in \mathbb{R}$ consider the supremum of drifted Brownian motion and its time, i.e.

$$M_{1/2}(T, a) := \sup_{t \in [0, T]} \{B(t) - at\}, \quad \tau_{1/2}(T, a) := \arg \max_{t \in [0, T]} \{B(t) - at\}, \tag{9}$$

and their expected values

$$\mathcal{M}_{1/2}(T, a) := \mathbb{E}(M_{1/2}(T, a)), \quad \mathcal{E}_{1/2}(T, a) := \mathbb{E}(\tau_{1/2}(T, a)). \tag{10}$$

In the following, let $p(t, y; T, a)$ be the joint density of $(\tau_{1/2}(T, a), M_{1/2}(T, a))$, i.e.

$$p(t, y; T, a) := \frac{\mathbb{P}(\tau_{1/2}(T, a) \in dt, M_{1/2}(T, a) \in dy)}{dt dy}.$$

We note that $\tau_{1/2}(T, a)$ is well-defined (unique); see the comment below (14). When $T \in (0, \infty)$ and $a \in \mathbb{R}$ then

$$p(t, y; T, a) = \frac{y \exp\{-(y + ta)^2/2t\}}{\pi t^{3/2} \sqrt{T-t}} \left(e^{-a^2(T-t)/2} + a \sqrt{\frac{1}{2}\pi(T-t)} \operatorname{erfc}\left(-a \sqrt{\frac{1}{2}(T-t)}\right) \right) \tag{11}$$

for $t \in (0, T)$ and $y > 0$. When $a > 0$, then the pair $(\tau_{1/2}(\infty, a), M_{1/2}(\infty, a))$ is well-defined, with

$$p(t, y; \infty, a) = \frac{\sqrt{2} ay \exp\{-(y + ta)^2/2t\}}{t^{3/2} \sqrt{\pi}} \tag{12}$$

for $t > 0$ and $y > 0$.

Proposition 2.

(i) If $T \in (0, \infty)$ and $a \neq 0$ then

$$\begin{aligned} \mathcal{M}_{1/2}(T, a) &= \frac{1}{2a} \left(-a^2 T + (1 + a^2 T) \operatorname{erf}\left(a \sqrt{\frac{T}{2}}\right) + \sqrt{\frac{2T}{\pi}} \cdot a e^{-a^2 T/2} \right), \\ \mathcal{E}_{1/2}(T, a) &= \frac{1}{2a^2} \left(a^2 T + (1 - a^2 T) \operatorname{erf}\left(a \sqrt{\frac{T}{2}}\right) - \sqrt{\frac{2T}{\pi}} \cdot a e^{-a^2 T/2} \right); \end{aligned}$$

- (ii) if $a > 0$ then $\mathcal{M}_{1/2}(\infty, a) = 1/2a$ and $\mathcal{E}_{1/2}(\infty, a) = 1/2a^2$;
- (iii) if $T \in (0, \infty)$ then $\mathcal{M}_{1/2}(T, 0) = \sqrt{2T/\pi}$ and $\mathcal{E}_{1/2}(T, 0) = T/2$.

Proof. The fomula for $\mathcal{M}_{1/2}(T, a)$ can be obtained from the Laplace transform of $M_{1/2}(T, a)$; see [7, (1.1.1.3) and (2.1.1.3)]. The formula for $\mathcal{E}_{1/2}(T, a)$ could similarly be obtained from the Laplace transform of $\tau_{1/2}(T, a)$. However, numerical calculations indicate that the formulas for the Laplace transforms (1.1.12.3) and (2.1.12.3) in [7] are incorrect. Therefore, we provide our own derivation of $\mathcal{E}_{1/2}(T, a)$ in Appendix B (available in the Supplementary Material of the online version of this manuscript). □

Finally, we introduce a certain functional of Brownian motion, which plays an important role in this manuscript. We note that its special case ($H = \frac{1}{2}$) appeared in [5, (2.8)]. In what follows let $Y(t) := B(t) - at$ and

$$I_H(t, y) := \mathbb{E} \left(\int_0^t (t-s)^{H-(3/2)} (Y(t) - Y(s)) ds \mid \tau_{1/2}(T, a) = t, M_{1/2}(T, a) = y \right). \quad (13)$$

Following [5], we recognise that the conditional distribution of the process $\{Y(t) - Y(t-s) : s \in [0, t]\}$ given $(\tau_{1/2}(T, a), M_{1/2}(T, a)) = (t, y)$ follows the law of the generalised three-dimensional Bessel bridge from (0,0) to (t, y). Therefore, $I_H(t, y)$ can be thought of as an expected value of a certain ‘Brownian area’; see [14] for a survey on Brownian areas. It turns out that the function $I_H(t, y)$ can be explicitly calculated. In the following, $U(a, b, z)$ is Tricomi’s confluent hypergeometric function; see (23) in Appendix A.

Lemma 1. *If $H \in (0, \frac{1}{2}) \cup (\frac{1}{2}, 1)$ and $t, y > 0$, then*

$$I_H(t, y) = \frac{t^{H+(1/2)}}{y(H - \frac{1}{2})(H + \frac{1}{2})} \left(1 - \frac{\Gamma(H)}{\sqrt{\pi}} U \left(H - \frac{1}{2}, \frac{1}{2}, \frac{y^2}{2t} \right) \right) + \frac{t^{H-(1/2)}y}{H + \frac{1}{2}}.$$

Proof of Lemma 1. Let

$$g(x, s; t, y) := \frac{\mathbb{P}(Y(t) - Y(t-s) \in dx \mid (\tau_{1/2}(T, a), M_{1/2}(T, a)) = (t, y))}{dx}.$$

From [5, (2.7)] we have

$$g(x, s; t, y) = \frac{(x/s^{3/2}) \exp\{-x^2/2s\}}{(y/t^{3/2}) \exp\{-y^2/2t\}} \cdot \frac{1}{\sqrt{2\pi(t-s)}} \left[\exp \left\{ -\frac{(y-x)^2}{2(t-s)} \right\} - \exp \left\{ -\frac{(y+x)^2}{2(t-s)} \right\} \right]$$

for $x > 0$. Using the Fubini–Tonelli theorem we have

$$I_H(t, y) = \int_0^t \int_0^\infty s^{H-3/2} x \cdot g(x, s; t, y) dx ds.$$

The rest of the proof is purely calculational. For completeness, it is given in Appendix B (available in the Supplementary Material of the online version of this manuscript). □

3. Main results

Let $\{B(t) : t \in \mathbb{R}\}$ be a standard, two-sided Brownian motion. Consider the PWZ representation of linear fractional Brownian motion with parameter $c \in \mathbb{R}_0^2$, i.e. $\{\tilde{B}_H^c(t) : t \in \mathbb{R}^+\}$, where

$$\tilde{B}_H^c(t) := \frac{\tilde{X}_H^c(t)}{\sqrt{V_H^c}},$$

with $\tilde{X}_H^c(t)$ defined in (8) and V_H^c defined in (4). Then, according to Corollary 1, $\{\tilde{B}_H^c(t) : H \in (0, 1) \times \mathbb{R}_+\}$ is a continuous modification of $\{B_H^c(t) : H \in (0, 1) \times \mathbb{R}_+\}$ and therefore, for each fixed H , $\{\tilde{B}_H^c(t) : t \in \mathbb{R}_+\}$ is a fractional Brownian motion with Hurst index H . We note that all the processes \tilde{B}_H^c live in the same probability space and are, in fact, defined pathwise for every realisation of the driving Brownian motion.

For each $c \in \mathbb{R}_0^2$, $a \in \mathbb{R}$, and $T > 0$ define

$$M_H^c(T, a) := \sup_{t \in [0, T]} \{B_H^c(t) - at\}, \quad \tau_H^c(T, a) := \arg \max_{t \in [0, T]} \{B_H^c(t) - at\}, \tag{14}$$

which is the supremum of the drifted fractional Brownian motion with parameter c and its location. We note that $\tau_H^c(T, a)$ is well-defined (almost surely unique); see [12]. Now we define the expected values of the supremum,

$$\mathcal{M}_H(T, a) := \mathbb{E}(M_H^c(T, a)) = \mathbb{E}(B_H^c(\tau_H^c(T, a)) - a\tau_H^c(T, a)).$$

Recall that in the case $c = (1, 0)$ and $H = \frac{1}{2}$, the random variables and their expectations were already defined in (9) and (10). Notice how $\mathcal{M}_H(T, a)$ does not depend on c , because as c varies, the law of the supremum does not change.

3.1. The lower bound

We now proceed to derive the lower bound for $\mathcal{M}_H(T, a)$. The final result is provided in Theorem 1 at the end of this subsection. All proofs are provided in Section 5.

For each $c \in \mathbb{R}_0^2$ define

$$m_H^c(T, a) := \mathbb{E}(\tilde{B}_H^c(\tau_{1/2}(T, a)) - a\tau_{1/2}(T, a)), \tag{15}$$

which, in words, is the expected value of the drifted fractional Brownian motion with parameter c evaluated at the time of the supremum of the driving Brownian motion $\tau_{1/2}(T, a)$ defined in (9). Clearly, this yields a lower bound for the expected supremum, i.e. $\mathcal{M}_H(T, a) \geq m_H^c(T, a)$. We can further maximise our lower bound by taking the supremum over all $c \in \mathbb{R}_0^2$ and define $m_H(T, a) := \sup_{c \in \mathbb{R}_0^2} m_H^c(T, a)$. It turns out that the value of $m_H(T, a)$ can be found explicitly. Before showing that formula in Proposition 4, we define the useful functionals

$$\mathcal{J}_H(T, a) := \mathbb{E}\{X_H^+(\tau_{1/2}(T, a))\}, \quad \mathcal{J}_H^-(T, a) := \mathbb{E}\{X_H^-(\tau_{1/2}(T, a))\}. \tag{16}$$

Lemma 2. *If $T \in (0, \infty)$ and $a \in \mathbb{R}$ then $\mathcal{J}_H^-(T, a) = -\mathcal{J}_H(T, -a)$.*

The proof of Lemma 2 is given in Section 5. In the following, $\gamma(\alpha, z)$ is the incomplete Gamma function; see (31) in Appendix A.

Proposition 3.

$$\mathcal{J}_H(T, a) = \begin{cases} \frac{2^H}{\sqrt{2\pi}(H+\frac{1}{2})} \cdot |a|^{-2H} \gamma(H, a^2T/2), & a \neq 0, T \in (0, \infty); \\ \frac{2^H \Gamma(H)}{\sqrt{2\pi}(H+\frac{1}{2})} \cdot |a|^{-2H}, & a > 0, T = \infty; \\ \frac{T^H}{\sqrt{2\pi}H(H+\frac{1}{2})}, & a = 0, T \in (0, \infty). \end{cases}$$

Finally, we can show the following.

Proposition 4. *If $a \in \mathbb{R}$ and $T \in (0, \infty)$ or $a > 0$ and $T = \infty$, then*

$$m_H^c(T, a) = \frac{c_+ - c_-}{\sqrt{V_H^c}} \cdot \mathcal{J}_H(T, a) - a\mathcal{E}_{1/2}(T, a) \tag{17}$$

and

$$m_H(T, a) = m_H^{(1,-1)}(T, a) = \frac{\mathcal{J}_H(T, a)}{C_H \sin\left(\frac{1}{2}\pi\left(H + \frac{1}{2}\right)\right)} - a\mathcal{E}_{1/2}(T, a),$$

with V_H^c and C_H defined in (4) and (5), respectively.

We emphasise that the values of $\mathcal{E}_{1/2}(T, a)$ and $\mathcal{J}_H(T, a)$ are known; see Propositions 2 and 3 respectively.

We can further improve the lower bound derived in Proposition 4 simply by using the self-similarity of fractional Brownian motion. For any $\rho > 0$ we have $\mathcal{M}_H(T, a) = \rho^{-H} \mathcal{M}_H(\rho T, \rho^{H-1}a)$, which also holds for $a > 0$ and $T = \infty$, i.e. $\mathcal{M}_H(\infty, a) = \rho^{-H} \mathcal{M}_H(\infty, \rho^{H-1}a)$.

Finally, let

$$\underline{\mathcal{M}}_H(T, a) := \sup_{\rho > 0} \{\rho^{-H} m_H(\rho T, \rho^{H-1}a)\}. \tag{18}$$

Theorem 1. *For any $H \in (0, 1)$, $T > 0$, and $a \in \mathbb{R}$, $\mathcal{M}_H(T, a) \geq \underline{\mathcal{M}}_H(T, a)$.*

For general (T, a) , the solution to the optimisation problem (18) can be found numerically. We were able to determine the value of $\underline{\mathcal{M}}_H(T, a)$ explicitly in two special cases, which we display in the following corollary. For convenience, we also provide the corresponding values of $m_H(T, a)$.

Corollary 2. *For $H \in (0, 1)$, with C_H defined in (5),*

(i) *if $T \in (0, \infty)$, then*

$$\underline{\mathcal{M}}_H(T, 0) = m_H(T, 0) = \frac{T^H}{\sqrt{2\pi} C_H H (H + \frac{1}{2}) \sin\left(\frac{1}{2}\pi\left(H + \frac{1}{2}\right)\right)};$$

(ii) *if $a > 0$, then*

$$\underline{\mathcal{M}}_H(\infty, a) = \frac{1 - H}{2aH} \left(\frac{2^{H+1} a^{1-2H} H \Gamma(H)}{\sqrt{2\pi} C_H (H + \frac{1}{2}) \sin\left(\frac{1}{2}\pi\left(H + \frac{1}{2}\right)\right)} \right)^{1/(1-H)},$$

$$m_H(\infty, a) = \frac{2^H \Gamma(H)}{\sqrt{2\pi} C_H a^{2H} (H + \frac{1}{2}) \sin\left(\frac{1}{2}\pi\left(H + \frac{1}{2}\right)\right)} - \frac{1}{2a}.$$

The proof of Corollary 2 relies solely on simple algebraic manipulations.

3.2. Secondary results

Before ending this section, we would like to present two immediate corollaries that are implied by our main results. The first result describes the asymptotic behavior of $\mathcal{M}_H(T, 0)$ as $H \downarrow 0$, while the second result pertains to the evaluation of the derivative of the expected supremum $\mathcal{M}_H(T, a)$ at $H = \frac{1}{2}$.

3.2.1. *Behavior of $\underline{\mathcal{M}}_H(1, 0)$ as $H \downarrow 0$* Using the formula for $\underline{\mathcal{M}}_H(T, 0)$ from Theorem 1(i), it is easy to obtain the following result.

Corollary 3.

$$\underline{\mathcal{M}}_H(1, 0) \sim \frac{2}{\sqrt{\pi H}}, \quad H \rightarrow 0.$$

The asymptotic lower bound in Corollary 3 is over five times larger than the corresponding bound derived in [8, Theorem 2.1(i)], where it was shown that $\mathcal{M}_H(1, 0) \geq (4H\pi e \log(2))^{-1/2}$ for all $H \in (0, 1)$. Moreover, together with [9, Corollary 2], our result implies that $1.128 \leq H^{-1/2} \cdot \mathcal{M}_H(1, 0) \leq 1.695$ for all H small enough. Determining whether the limit $H^{-1/2} \cdot \mathcal{M}_H(1, 0)$ as $H \rightarrow 0$ exists and finding its value remain interesting open questions.

3.2.2. *Derivative of the expected supremum.* Recently, [5] considered the derivative of the expected supremum with respect to the Hurst parameter at $H = \frac{1}{2}$, that is $\mathcal{M}'_{1/2}(T, a) := (\partial/\partial H)\mathcal{M}_H(T, a)|_{H=1/2}$. In [5, Theorem 3.1], they derived an expression for $\mathcal{M}'_{1/2}(T, a)$ in terms of a definite double integral and in [5, Corollary 3.3] they derived a more explicit result in two special cases $a = 0$ and $T = \infty$. Using the formula for $\mathcal{J}_H(T, a)$ we established in Proposition 3, we are able to explicitly evaluate the derivative in the general case. In the following, let $\gamma'(s, x) = (\partial/\partial s)\gamma(s, x)$.

Theorem 2.

$$\mathcal{M}'_{1/2}(T, a) = \frac{1}{\sqrt{\pi}|a|} \left(\log(2a^{-2})\gamma\left(\frac{1}{2}, \frac{a^2T}{2}\right) + \gamma'\left(\frac{1}{2}, \frac{a^2T}{2}\right) \right).$$

Note that the continuous extension of the function $\mathcal{M}'_{1/2}(T, a)$ to $(T, 0)$ and (∞, a) agrees with [5, Corollary 3.3].

Proof of Theorem 2. The proof of [5, Theorem 3.1] implies that

$$\mathcal{M}'_{1/2}(T, a) := \frac{\partial}{\partial H} \mathcal{M}_H(T, a) \Big|_{H=1/2} = \frac{\partial}{\partial H} m_H^{(1,0)}(T, a) \Big|_{H=1/2}.$$

Therefore, using the formula for $m_H^{(1,0)}(T, a)$ from Proposition 4, we find that $\mathcal{M}'_{1/2}(T, a) = \mathcal{J}_{1/2}(T, a) + (\partial/\partial H)\mathcal{J}_H(T, a)|_{H=1/2}$. The proof is concluded after simple algebraic manipulations. □

4. Numerical experiments

In this section we compare our theoretical lower bound $\underline{\mathcal{M}}_H(T, a)$ with Monte Carlo simulations.

In our experiments we use the circulant embedding method (also called the Davies–Harte method [10]) for simulating fractional Brownian motion; see also [11] for various methods of simulation. Experiments were performed in Python, and the code for the Davies–Harte method was adapted from [16, Section 12.4.2]. The method relies on the simulation of fractional Brownian motion on an equidistant grid of n points, i.e. $(B(0), B(T/n), B(2T/n), \dots, B(T))$. The resulting estimator has the expected value $\mathcal{M}_H^n(T, a) := \mathbb{E}(\sup_{t \in \mathcal{T}_n} \{B_H(t) - at\})$, where $\mathcal{T}_n := \{0, T/n, 2T/n, \dots, T\}$. Clearly, $\mathcal{M}_H^n(T, a) \leq \mathcal{M}_H(T, a)$; i.e., on average, the Monte Carlo estimator underestimates the ground truth, as the supremum is taken over a finite subset of $[0, T]$. Nonetheless, as $n \rightarrow \infty$, $\mathcal{M}_H^n(T, a) \rightarrow \mathcal{M}_H(T, a)$.

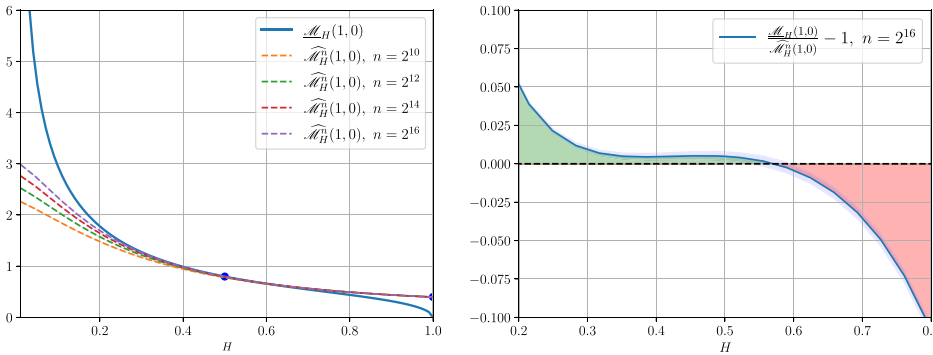


FIGURE 1. Numerical results for the case $T = 1, a = 0$.

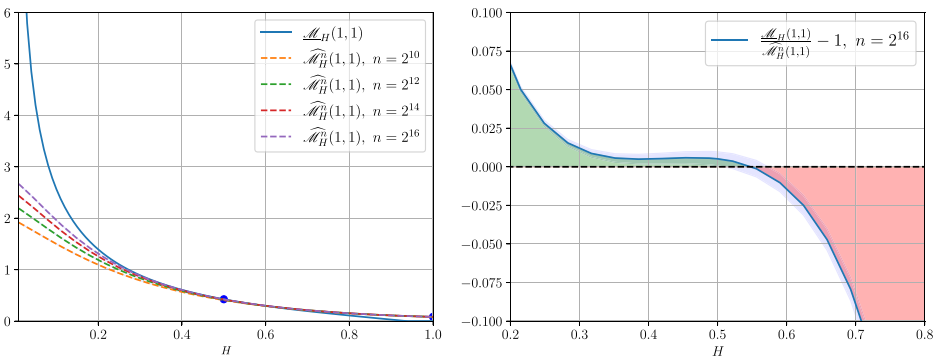


FIGURE 2. Numerical results for the case $T = 1, a = 1$.

In our experiments, we consider three different cases: (i) $T = 1, a = 0$; (ii) $T = 1, a = 1$; and, finally, (iii) $T = \infty, a = 1$. In each case the theoretical lower bound $\mathcal{M}_H(T, a)$ is compared with the corresponding simulation results $\widehat{\mathcal{M}}_H^n(T, a)$ for $n \in \{2^{10}, 2^{12}, 2^{14}, 2^{16}\}$ based on 20 000 independent runs of the Davies–Harte algorithm; in case (ii) we took $T = 10$ because it is not possible to simulate the process over the infinite time horizon.

The results corresponding to cases (i)–(iii) are displayed in Figs. 1–3. Each curve is surrounded by its 95% confidence interval depicted as a shaded blue area. The results are presented in two different scales. We interpret the results on the figures on the left and on the right separately, in the following two paragraphs.

In the figures on the left, we compare the bound with the simulation results on the ‘high’ level for all $H \in (0.01, 1)$. The blue dots at $H = \frac{1}{2}$ and $H = 1$ correspond to the known values of $\mathcal{M}_{1/2}(T, a)$ and $\mathcal{M}_1(T, a)$ respectively; the value at $H = 1$ in Fig. 3 is not shown because $\mathcal{M}_1(\infty, 1) = \infty$. As expected, the value of $\widehat{\mathcal{M}}_H^n(T, a)$ is increasing, as n is increasing. The simulation results seem to roughly agree with the ground truth at $H = \frac{1}{2}$ and $H = 1$, while the lower bound agrees with the ground truth at $H = \frac{1}{2}$ by definition, i.e. $\mathcal{M}_{1/2}(T, a) = \mathcal{M}_{1/2}(T, a)$. On the ‘high’ level, we can conclude that the lower bound $\underline{\mathcal{M}}_H(T, a)$

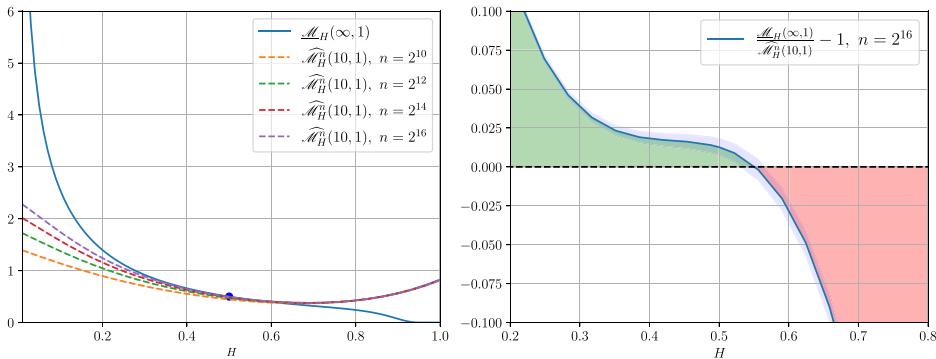


FIGURE 3. Numerical results for the case $T = \infty, a = 1$.

- is close to the simulation results for all $H \approx \frac{1}{2}$;
- performs much better than the simulation results as $H \rightarrow 0$; and
- performs worse when $H \rightarrow 1$ (in fact, the bound seems to converge to 0 there).

On the right of the figures, we compare the bound with the simulation results in the region $H \in (0.2, 0.8)$. We show the relative error between the theoretical lower bound and the simulation results based on $n = 2^{16}$ grid points, i.e. $(\mathcal{M}_H(T, a) - \widehat{\mathcal{M}}_H^n(T, a)) / \widehat{\mathcal{M}}_H^n(T, a)$. We note that if the relative error is positive, then the theoretical lower bound yields a *better approximation* to the ground truth than the Monte Carlo method, which is indicated by the green area below the curve on the plot. In this sense, we see that the theoretical lower bound outperforms the Monte Carlo simulations for $H \in (0, \frac{1}{2})$ in all three cases (i)–(iii). We remark that the value of the relative error at $H = \frac{1}{2}$ approximately equals 0.5% in Fig. 1 and 0.7% in Fig. 2; this roughly agrees with [6, Corollary 4.3], which states that

$$\mathcal{M}_{1/2}^n(T, a) - \mathcal{M}_{1/2}(T, a) \approx -\sqrt{T} \cdot \frac{\zeta(1/2)}{\sqrt{2\pi n}} \approx -0.5826 \cdot \sqrt{T/n},$$

where $\zeta(\cdot)$ is the Riemann zeta function. See also [2, Theorem 2] for the case $a = 0$.

5. Proofs

Here we provide proofs of Lemma 2, Proposition 3, and Proposition 4 from Section 3.1.

Proof of Lemma 2. For brevity we write $\tau := \tau_{1/2}(T, a)$ and put $Y(t) := B(t) - at$. According to the PWZ representation of \tilde{X}_H^+ in (7), we have

$$\begin{aligned} \mathbb{E}(\tilde{X}_H^+(\tau)) &= \mathbb{E}\left(\tau^{H-(1/2)}B(\tau) - (H - (1/2)) \cdot \int_0^\tau (\tau - s)^{H-(3/2)} \cdot (B(\tau) - B(s)) ds\right) \\ &= \mathbb{E}\left(\tau^{H-(1/2)}Y(\tau) + \frac{a\tau^{H+(1/2)}}{H + 1/2} - (H - \frac{1}{2}) \cdot \int_0^\tau (\tau - s)^{H-(3/2)} \cdot (Y(\tau) - Y(s)) ds\right), \end{aligned} \tag{19}$$

where in the second line we simply substituted $B(t) = Y(t) + at$ and integrated out $\int_0^\tau (\tau - s)^{H-(3/2)}(a\tau - as) ds$. Furthermore, notice that for any $T \in (0, \infty)$, the PWZ representation of

$\tilde{X}_H^-(\tau)$ from (7) can be rewritten as

$$\begin{aligned} \tilde{X}_H^-(\tau) := & -(T - \tau)^{H-(1/2)}(B(\tau) - B(T)) + (H - \frac{1}{2}) \cdot \int_{\tau}^T (s - \tau)^{H-(3/2)}(B(\tau) - B(s)) \, ds \\ & + (H - \frac{1}{2}) \cdot \int_0^T s^{H-(3/2)}B(s) \, ds - T^{H-(1/2)}B(T) \\ & + (H - \frac{1}{2}) \cdot \int_T^{\infty} [s^{H-(3/2)} - (s - \tau)^{H-(3/2)}] \cdot (B(s) - B(T)) \, ds. \end{aligned}$$

Since Brownian motion is centred and has independent increments, τ is independent of $\{B(T + s) - B(T) : s > 0\}$ and the expected value of each term in the second and third lines above is equal to 0. This yields

$$\begin{aligned} \mathbb{E}(\tilde{X}_H^-(\tau)) &= -\mathbb{E}\left((T - \tau)^{H-(1/2)}(B(\tau) - B(T)) - (H - \frac{1}{2}) \cdot \int_{\tau}^T (s - \tau)^{H-(3/2)}(B(\tau) - B(s)) \, ds \right). \end{aligned}$$

After substituting $B(t) = Y(t) + at$ we find that this equals

$$\begin{aligned} & -\mathbb{E}\left((T - \tau)^{H-(1/2)}(Y(\tau) - Y(T)) \right. \\ & \left. - \frac{a(T - \tau)^{H+(1/2)}}{H + 1/2} - (H - \frac{1}{2}) \cdot \int_{\tau}^T (s - \tau)^{H-(3/2)}(Y(\tau) - Y(s)) \, ds \right). \end{aligned}$$

Now let $\{\hat{Y}(t) : t \in [0, T]\}$ be the time-reverse of process Y , i.e. $\hat{Y}(t) := Y(T - t) - Y(T)$, and let $\hat{\tau} := \arg \max\{t \in [0, T] : \hat{Y}(t)\}$ be the time of its supremum over $[0, T]$. Notice that we must have $\tau^* = T - \tau$. After substituting for \hat{Y} , we find that

$$\mathbb{E}(\tilde{X}_H^-(\tau)) = -\mathbb{E}\left(\hat{\tau}^{H-(1/2)}\hat{Y}(\tau) - \frac{a\hat{\tau}^{H+(1/2)}}{H + 1/2} - (H - \frac{1}{2}) \cdot \int_0^{\hat{\tau}} (\hat{\tau} - s)^{H-(3/2)}(\hat{Y}(\tau) - \hat{Y}(s)) \, ds \right).$$

Finally, we notice that $\hat{Y}(\cdot) \stackrel{d}{=} Y(\cdot; -a)$, i.e. \hat{Y} follows the law of drifted Brownian motion with drift $-a$. Comparing the above with (19) for $\mathbb{E}\tilde{X}_H^+(\tau)$ concludes the proof. □

In light of the result in Lemma 2 the function $\mathcal{J}_H^-(T, a)$ can be expressed using $\mathcal{J}_H(T, a)$, which justifies our notation $\mathcal{J}_H(T, a)$ instead of $\mathcal{J}_H^+(T, a)$, cf. (16). Before proving Proposition 3, we need to establish a certain continuity property of the argmax functional of Brownian motion. In what follows, let $\tau_{1/2}(T, a) := \arg \max_{t \in [0, T]} \{B(t) - at\}$ be the argmax functional of drifted Brownian motion; see also the definition in (14).

Lemma 3.

- (i) $\lim_{a \rightarrow a^*} \tau_{1/2}(T, a) = \tau_{1/2}(T, a^*)$ a.s. for any $T \in (0, \infty)$, $a^* \in \mathbb{R}$.
- (ii) $\lim_{T \rightarrow \infty} \tau_{1/2}(T, a) = \tau_{1/2}(\infty, a)$ a.s. for any $a > 0$.

Proof. Let $Y(t; a) := B(t) - at$. It is easy to see that the trajectories $\{Y(t, a) : t \in [0, T]\}$ converge uniformly to $\{Y(t, a^*) : t \in [0, T]\}$ as $a \rightarrow a^*$, and hence the argmax functionals also

converge; see, e.g., [22, Lemma 2.9], which concludes the proof of item (i). Furthermore, since $\tau_{1/2}(\infty, a)$ is almost surely finite, then there must exist some (random) $T_0 > 0$ such that $\tau_{1/2}(T, a) = \tau_{1/2}(\infty, a)$ for all $T > T_0$, which implies item (ii). \square

Proof of Proposition 3. Consider the case $H = \frac{1}{2}$. Since the value of $\mathcal{M}_{1/2}(T, a)$ is irrespective of c (see also the comment above (15)), we may take $c = (1, 0)$ and observe that

$$\begin{aligned} \mathcal{M}_{1/2}(T, a) &= \mathbb{E}(M_{1/2}^{(1,0)}(T, a)) = \mathbb{E}(B_{1/2}^{(1,0)}(\tau_{1/2}(T, a)) - a\tau_{1/2}(T, a)) \\ &= \frac{\mathbb{E}(\tilde{X}_{1/2}^+(\tau(T, a)))}{\sqrt{V_{1/2}^{(1,0)}}} - a\mathbb{E}(\tau_{1/2}(T, a)) \\ &= \mathcal{J}_{1/2}(T, a) - a\mathcal{E}_{1/2}(T, a); \end{aligned}$$

therefore $\mathcal{J}_{1/2}(T, a) = \mathcal{M}_{1/2}(T, a) + a\mathcal{E}_{1/2}(T, a)$, which agrees with Proposition 2 (note that the error function is a special case of the incomplete Gamma function, cf. (34)).

Now let $H \in (0, \frac{1}{2}) \cup (\frac{1}{2}, 1)$. For brevity, we write $\tau := \tau_{1/2}(T, a)$ and let $Y(t) = B(t) - at$. We now consider the case $T \in (0, \infty)$, $a \neq 0$. Recall that, from (19), we have

$$\mathcal{J}_H(T, a) = \mathbb{E}\left(\tau^{H-\frac{1}{2}}Y(\tau) + \frac{a\tau^{H+(1/2)}}{H+1/2} - (H-\frac{1}{2}) \cdot \int_0^\tau (\tau-s)^{H-(3/2)} \cdot (Y(\tau) - Y(s)) ds\right).$$

Now, we have

$$\begin{aligned} &\mathbb{E}\left(\int_0^\tau (\tau-s)^{H-(3/2)} \cdot (Y(\tau) - Y(s)) ds\right) \\ &= \mathbb{E}\left(\mathbb{E}\left(\int_0^t (t-s)^{H-(3/2)} \cdot (Y(t) - Y(s)) ds \mid \tau = t, Y(\tau) = y\right)\right). \end{aligned}$$

We now recognise that the above equals $\mathbb{E}(I_H(\tau, Y(\tau)))$, with $I_H(t, y)$ defined in (13). Using Lemma 1 we obtain $\mathcal{J}_H(T, a) = \mathcal{J}_H^{(1)}(T, a) + \mathcal{J}_H^{(2)}(T, a)$, where

$$\begin{aligned} \mathcal{J}_H^{(1)}(T, a) &:= \frac{1}{H+1/2} \cdot \mathbb{E}\left(\tau^{H-(1/2)}\left(Y(\tau) + a\tau - \frac{\tau}{Y(\tau)}\right)\right), \\ \mathcal{J}_H^{(2)}(T, a) &:= \frac{1}{H+1/2} \cdot \mathbb{E}\left(\frac{\tau^{H+(1/2)}}{Y(\tau)} \cdot \frac{\Gamma(H)}{\sqrt{\pi}} U\left(H - \frac{1}{2}, \frac{1}{2}, \frac{Y^2(\tau)}{2\tau}\right)\right). \end{aligned}$$

The joint density of the pair $(\tau, Y(\tau))$ is well known (see (11) in Section 2.2) and therefore both functions $\mathcal{J}_H^{(1)}(T, a)$ and $\mathcal{J}_H^{(2)}(T, a)$ can be written as definite integrals and calculated. In fact, we have

$$\mathcal{J}_H^{(1)}(T, a) = 0, \quad \mathcal{J}_H^{(2)}(T, a) = \frac{2^H}{\sqrt{2\pi}(H+1/2)} \cdot |a|^{-2H} \gamma\left(H, \frac{a^2T}{2}\right). \tag{20}$$

The derivation of (20) is purely calculational and is provided in Appendix B (available in the Supplementary Material of the online version of this manuscript). This ends the proof in the case $T \in (0, \infty)$, $a \neq 0$.

In order to derive the formula for $\mathcal{J}_H(T, a)$ in the remaining two cases (i.e. $T \in (0, \infty), a = 0$ and $T = \infty, a > 0$), we could redo the calculations in (20) with appropriate density functions for the pair $(\tau, Y(\tau))$; see (12) and (11). However, this is not necessary, as it suffices to show that the function $\mathcal{J}_H(T, a)$ is continuous at (∞, a) and $(T, 0)$.

Let $T \in (0, \infty), a = 0$. Using the fact that $\gamma(s, x) \sim (sx^s)^{-1}$ as $x \downarrow 0$, we can see that

$$\lim_{a \rightarrow 0} \mathcal{J}_H(T, a) = \frac{T^H}{\sqrt{2\pi}H(H + 1/2)}.$$

Showing that $\lim_{a \rightarrow 0} \mathcal{J}_H(T, a) = \mathcal{J}_H(T, 0)$ would therefore conclude the proof in this case. By definition we have $\mathcal{J}_H(T, a) = \sqrt{V(H)} \cdot \mathbb{E}(B_H^{(1,0)}(\tau(T, a)))$. Since $V(H)$ is continuous at $H = \frac{1}{2}$, it suffices to show that

$$\mathbb{E}(B_H^{(1,0)}(\tau(T, a))) \rightarrow \mathbb{E}(B_H^{(1,0)}(\tau(T, 0))) \tag{21}$$

as $a \rightarrow 0$. Using Proposition 1 and Lemma 3(i), we obtain

$$\lim_{a \rightarrow 0} B_H^{(1,0)}(\tau(T, a)) = B_H^{(1,0)}(\tau(T, 0)) \quad \text{a.s.}$$

Moreover, for any $\varepsilon > 0$ and all $a \in (-\varepsilon, \varepsilon)$ we have

$$B_H^{(1,0)}(\tau(T, a)) \leq \sup_{t \in [0, T]} B_H^{(1,0)}(t) + \varepsilon T,$$

which has finite expectation. Therefore, by Lebesgue dominated convergence we can conclude that the limit in (21) holds, which ends the proof in this case.

Let $T = \infty, a > 0$. It is easy to see that

$$\lim_{T \rightarrow \infty} \mathcal{J}_H(T, a) = \frac{2^H \Gamma(H)}{\sqrt{2\pi}(H + 1/2)} \cdot |a|^{-2H} \quad \text{if } a > 0.$$

Analogously to the proof of the previous case, it suffices to show that

$$\mathbb{E}(B_H^{(1,0)}(\tau(T, a))) \rightarrow \mathbb{E}(B_H^{(1,0)}(\tau(\infty, a))) \tag{22}$$

as $T \rightarrow \infty$. Using Proposition 1 and Lemma 3(ii), we find that

$$\lim_{T \rightarrow \infty} B_H^{(1,0)}(\tau(T, a)) = B_H^{(1,0)}(\tau(\infty, a)) \quad \text{a.s.}$$

Moreover, since the mapping $T \mapsto \tau(T, a)$ is non-decreasing, we have

$$B_H^{(1,0)}(\tau(T, a)) \leq M_H^{(1,0)}(\infty, a) + a\tau(\infty, a),$$

and the right-hand side above has a finite expectation. Using Lebesgue dominated convergence we conclude that the limit (22) holds, which ends the proof. \square

Proof of Proposition 4. From the definition of $m_H^c(T, a)$ in (15),

$$m_H^c(T, a) := \mathbb{E}\{\tilde{B}_H^c(\tau(T, a)) - a\tau(T, a)\} = \frac{c_+ \mathcal{J}_H^+(T, a) - c_- \mathcal{J}_H^-(T, a)}{\sqrt{V_H^c}} - a\mathcal{E}_{1/2}(T, a).$$

In the light of Lemma 2, for $T \in (0, \infty)$ we have (17). We now show that (17) also holds in the case $T = \infty, a > 0$. Using Proposition 1 and Lemma 3(ii), we find that

$$\tilde{B}_H^c(\tau(T, a)) - a\tau(T, a) \rightarrow \tilde{B}_H^c(\tau(\infty, a)) - a\tau(\infty, a) \quad \text{a.s., } T \rightarrow \infty.$$

Now we have the bound $\tilde{B}_H^c(\tau(T, a)) - a\tau(T, a) \leq M_H^c(\infty, a)$, which is integrable, and hence we can conclude that $m_H^c(\infty, a) = \lim_{T \rightarrow \infty} m_H^c(T, a)$. Furthermore, from Propositions 3 and 2 it is clear that $\mathcal{J}_H(T, a) \rightarrow \mathcal{J}_H(\infty, a)$ and $\mathcal{E}_{1/2}(T, a) \rightarrow \mathcal{E}_{1/2}(\infty, a)$ as $T \rightarrow \infty$. Hence,

$$\lim_{T \rightarrow \infty} m_H^c(T, a) = \frac{c_+ - c_-}{\sqrt{V_H^c}} \cdot \mathcal{J}_H(T, a) - a\mathcal{E}_{1/2}(T, a),$$

which concludes the proof that (17) holds for all admissible pairs (T, a) .

Finally, since $J_H(T, a) > 0$ (see Proposition 3), it is easy to see that (17) is maximized whenever $(c_+ - c_-)/\sqrt{V_H^c}$ is maximized. It is straightforward to show that the maximum is attained at $c = (1, -1)$, which concludes the proof. \square

Appendix A. Special functions

All of the definitions, formulae, and relations from this section can be found in [1].

A.1. Confluent hypergeometric functions

For any $a, z \in \mathbb{R}$ and $b \in \mathbb{R} \setminus \{0, -1, -2, \dots\}$ we define Kummer’s (confluent hypergeometric) function

$${}_1F_1(a, b, z) := \sum_{n=0}^{\infty} \frac{a^{(n)}z^n}{b^{(n)}n!},$$

where $a^{(n)}$ is the rising factorial, i.e. $a^{(0)} := 1$ and $a^{(n)} := a(a + 1) \cdots (a + n - 1)$ for $n \in \mathbb{N}$. Similarly, for any $a, z \in \mathbb{R}$ and $b \in \mathbb{R} \setminus \{0, -1, -2, \dots\}$ we define Tricomi’s (confluent hypergeometric) function

$$U(a, b, z) = \frac{\Gamma(1 - b)}{\Gamma(a + 1 - b)} {}_1F_1(a, b, z) + \frac{\Gamma(b - 1)}{\Gamma(a)} {}_1F_1(a + 1 - b, 2 - b, z). \tag{23}$$

When $b > a > 0$, Kummer’s function can be represented as an integral,

$${}_1F_1(a, b, z) = \frac{\Gamma(b)}{\Gamma(a)\Gamma(b - a)} \int_0^1 e^{zt}t^{a-1}(1 - t)^{b-a-1} dt; \tag{24}$$

similarly, for $a > 0, z > 0$, Tricomi’s function can be represented as an integral,

$$U(a, b, z) = \frac{1}{\Gamma(a)} \int_0^{\infty} e^{-zt}t^{a-1}(1 + t)^{b-a-1} dt. \tag{25}$$

Moreover, we have the Kummer transformations

$${}_1F_1(a, b, z) = e^z {}_1F_1(b - a, b, -z), \tag{26}$$

$$U(a, b, z) = z^{1-b}U(1 + a - b, 2 - b, z) \tag{27}$$

and the recurrence relations

$$zU(a, b + 1, z) = (b - a)U(a, b, z) + U(a - 1, b, z), \tag{28}$$

$$aU(a + 1, b, z) = U(a, b, z) - U(a, b - 1, z). \tag{29}$$

In this manuscript we often use the following integral equality. Let $c > \gamma > 0$ and $u > 0$; then

$$\int_0^1 x^{\gamma-1}(1-x)^{c-\gamma-1} {}_1F_1(a, \gamma, ux) dx = \frac{\Gamma(\gamma)\Gamma(c-\gamma)}{\Gamma(c)} {}_1F_1(a, c, u), \tag{30}$$

which can be verified using [13, 7.613-1].

A.2. Incomplete Gamma function

For any $\alpha > 0, z > 0$, we define the *upper* and *lower* incomplete Gamma functions respectively as

$$\Gamma(\alpha, z) := \int_z^\infty t^{\alpha-1} e^{-t} dt, \quad \gamma(\alpha, z) := \int_0^z t^{\alpha-1} e^{-t} dt, \tag{31}$$

so that $\Gamma(\alpha, z) + \gamma(\alpha, z) = \Gamma(\alpha)$, where $\Gamma(\cdot)$ the standard Gamma function $\Gamma(\alpha) := \int_0^\infty t^{\alpha-1} e^{-t} dt$. Using integration by parts we obtain the useful recurrence relation

$$\gamma(\alpha + 1, z) = \alpha\gamma(\alpha, z) - z^\alpha e^{-z}. \tag{32}$$

Notice that, as $z \rightarrow \infty$, this is reduced to the well-known recurrence relation for the Gamma function, i.e. $\Gamma(\alpha + 1) = \alpha\Gamma(\alpha)$. Finally, we note that $\gamma(\alpha, z)$ can be expressed in terms of the confluent hypergeometric function:

$$\gamma(\alpha, z) = \alpha^{-1} z^\alpha e^{-z} {}_1F_1(1, \alpha + 1, z). \tag{33}$$

A.3. Error function

For $z \in \mathbb{R}$ we define the error function and complementary error function, respectively, as

$$\operatorname{erf}(z) := \frac{2}{\sqrt{\pi}} \int_0^z e^{-t^2} dt, \quad \operatorname{erfc}(z) := 1 - \operatorname{erf}(z).$$

The error function can be expressed in terms of the incomplete Gamma function, and therefore, in the light of (33), also in terms of the hypergeometric function:

$$\operatorname{erf}(z) = \frac{\operatorname{sgn}(z)}{\sqrt{\pi}} \gamma\left(\frac{1}{2}, z^2\right) = \frac{2ze^{-z^2}}{\sqrt{\pi}} {}_1F_1\left(1, \frac{3}{2}, z^2\right). \tag{34}$$

Acknowledgements

The author would like to thank Prof. Krzysztof Dębicki and Prof. Tomasz Rolski for helpful discussions, and the anonymous referees for their careful reading of the manuscript.

Funding information

Krzysztof Bisewski’s research was funded by SNSF Grant 200021-196888.

Competing interests

There were no competing interests to declare which arose during the preparation or publication process of this article.

Supplementary material

The Supplementary Material for this article, which contains Appendix B, can be found at <https://doi.org/10.1017/jpr.2022.129>.

References

- [1] ABRAMOWITZ, M. AND STEGUN, I. A. (1964). *Handbook of Mathematical Functions with Formulas, Graphs, and Mathematical Tables* (National Bureau of Standards Appl. Math. Ser. 55). U.S. Government Printing Office, Washington, D.C.
- [2] ASMUSSEN, S., GLYNN, P. AND PITMAN, J. (1995). Discretization error in simulation of one-dimensional reflecting Brownian motion. *Ann. Appl. Prob.* **5**, 875–896.
- [3] BENASSI, A., JAFFARD, S. AND ROUX, D. (1997). Elliptic Gaussian random processes. *Rev. Mat. Iberoamericana* **13**, 19–90.
- [4] BISEWSKI, K., DĘBICKI, K. AND MANDJES, M. (2021). Bounds for expected supremum of fractional Brownian motion with drift. *J. Appl. Prob.* **58**, 411–427.
- [5] BISEWSKI, K., DĘBICKI, K. AND ROLSKI, T. (2022). Derivatives of sup-functionals of fractional Brownian motion evaluated at $H = 1/2$. *Electron. J. Prob.* **27**, 1–35.
- [6] BISEWSKI, K. AND IVANOV, J. (2020). Zooming in on a Lévy process: Failure to observe threshold exceedance over a dense grid. *Electron. J. Prob.* **25**, 1–33.
- [7] BORODIN, A. N. AND SALMINEN, P. (2002). *Handbook of Brownian Motion—Facts and Formulae*, 2nd edn. Birkhäuser, Basel.
- [8] BOROVKOV, K., MISHURA, Y., NOVIKOV, A. AND ZHITLUKHIN, M. (2017). Bounds for expected maxima of Gaussian processes and their discrete approximations. *Stochastics* **89**, 21–37.
- [9] BOROVKOV, K., MISHURA, Y., NOVIKOV, A. AND ZHITLUKHIN, M. (2018). New and refined bounds for expected maxima of fractional Brownian motion. *Statist. Prob. Lett.* **137**, 142–147.
- [10] DAVIES, R. B. AND HARTE, D. (1987). Tests for Hurst effect. *Biometrika* **74**, 95–101.
- [11] DIEKER, T. (2004). Simulation of fractional Brownian motion. Master's thesis, Department of Mathematical Sciences, University of Twente.
- [12] FERGER, D. (1999). On the uniqueness of maximizers of Markov–Gaussian processes. *Statist. Prob. Lett.* **45**, 71–77.
- [13] GRADSHTEYN, I. S. AND RYZHIK, I. M. (2015). *Table of Integrals, Series, and Products*, 8th edn. Elsevier/Academic Press, Amsterdam.
- [14] JANSON, S. (2007). Brownian excursion area, Wright's constants in graph enumeration, and other Brownian areas. *Prob. Surv.* **4**, 80–145.
- [15] KORDZAKHIA, N. E., KUTOYANTS, Y. A., NOVIKOV, A. A. AND HIN, L.-Y. (2018). On limit distributions of estimators in irregular statistical models and a new representation of fractional Brownian motion. *Statist. Prob. Lett.* **139**, 141–151.
- [16] KROESE, D. P. AND BOTEV, Z. I. (2015). Spatial process simulation. In *Stochastic Geometry, Spatial Statistics and Random Fields*, ed. V. Schmidt. Springer, New York, pp. 369–404.
- [17] MAKOGIN, V. (2016). Simulation paradoxes related to a fractional Brownian motion with small Hurst index. *Mod. Stochastic Theory Appl.* **3**, 181–190.
- [18] MALSAGOV, A. AND MANDJES, M. (2019). Approximations for reflected fractional Brownian motion. *Phys. Rev. E* **100**, 032120.
- [19] MANDELBROT, B. B. AND VAN NESS, J. W. (1968). Fractional Brownian motions, fractional noises and applications. *SIAM Rev.* **10**, 422–437.
- [20] PELTIER, R.-F. AND VÉHEL, J. L. (1995). Multifractional Brownian motion: Definition and preliminary results. PhD thesis, INRIA.
- [21] SAMORODNITSKY, G. AND TAQQU, M. S. (1994). *Stable Non-Gaussian Random Processes*. Chapman & Hall, New York.
- [22] SEIJO, E. AND SEN, B. (2011). A continuous mapping theorem for the smallest argmax functional. *Electron. J. Statist.* **5**, 421–439.
- [23] SHAO, Q.-M. (1996). Bounds and estimators of a basic constant in extreme value theory of Gaussian processes. *Statist. Sinica* **6**, 245–257.

- [24] SHEPP, L. A. (1979). The joint density of the maximum and its location for a Wiener process with drift. *J. Appl. Prob.* **16**, 423–427.
- [25] STOEV, S. A. AND TAQQU, M. S. (2006). How rich is the class of multifractional Brownian motions? *Stochastic Process. Appl.* **116**, 200–221.
- [26] VARDAR-ACAR, C. AND BULUT, H. (2015). Bounds on the expected value of maximum loss of fractional Brownian motion. *Statist. Prob. Lett.* **104**, 117–122.